Isolation and Characterization of Actin and Actin-binding Protein from Human Platelets

SHARON ROSENBERG, ALFRED STRACHER, and ROGER C. LUCAS
Department of Biochemistry, State University of New York, Downstate Medical Center, Brooklyn, New York 11203

ABSTRACT   Human blood platelets, which are highly motile cells essential for the maintenance of hemostasis, contain large quantities of actin and other contractile proteins. We have previously introduced a method (Lucas, R. C., T. C. Detwiler, and A. Stracher, *J. Cell Biol.*, 1976, 70(2, Pt. 2):259 a) for the quantitative recovery of the platelets' cytoskeleton using a solution containing 1% Triton X-100 and 10 mM EGTA. This cytoskeleton contains most of the platelets' actin, actin-binding protein (ABP, subunit molecular weight = 260,000), and a 105,000-dalton protein. Negative staining of this Triton-insoluble residue on an EM grid shows it to consist of branched cables of actin filaments aligned in parallel.

When this cytoskeletal structure is dissolved in high-salt solutions, the actin and ABP dissociate and can subsequently be separated. Here we will present simple and rapid methods for the individual purifications of platelet actin and platelet ABP.

When purified actin and ABP are recombined in vitro, they are shown to be both necessary and sufficient for the reformation of the cytoskeletal complex. The reformed structure is visualized as a complex array of fibers, which at the EM level are seen to be bundles of actin filaments. The reformation of the cytoskeleton requires only that the actin be in the filamentous form—no accessory proteins, chelating agents, divalent cations, or energy sources are necessary.

In vivo, however, the state of assembly of the platelets' cytoskeleton appears to be under the control of the intracellular concentration of free calcium. Under conditions where proteolysis is inhibited and EGTA is omitted from the Triton-solubilization step, no cytoskeleton can be isolated. The ability of Ca^{+2} to control the assembly and disassembly of the platelets' cytoskeleton provides a mechanism for cytoskeletal involvement in shape change and pseudopod formation during platelet activation.

Human blood platelets are anucleate, discoid cells 2-3 μm in diameter. Under appropriate physiological stimuli, platelets undergo abrupt morphological changes to prevent bleeding from damaged blood vessels; the platelets change in shape from disks to spheres, send out long, slender filopodia, centralize their organelles, secrete the contents of their granules, aggregate with one another to form a hemostatic plug, and retract these aggregates (56). Contractile proteins have been implicated in most of these processes (1).

Crude actomyosin was originally isolated from platelets by Bettex-Galland and Lüscher in 1959 (4, 5) and was found to have many properties similar to those of actomyosins from other sources, including the ability to be dissociated into an actinlike and a myosinlike component. Filaments of these proteins have been difficult to identify and localize in thin sections of intact resting platelets because of the dense fibrogranular material filling the cytoplasmic matrix. However, electron micrographs of resting and stimulated platelets, after osmotic shock or glycerination to rarify the cytoplasm, show filaments distributed throughout the cytoplasm and filopodia (3, 57). Their ability to bind heavy meromyosin (HMM) identifies them as actin-containing microfilaments. The greater ratio of actin:myosin in nonmuscle cells than in muscle cells implies that actin in nonmuscle cells has more than just a contractile role, e.g., a cytoskeletal role.

In 1976, we introduced a procedure for the direct isolation, from human blood platelets, of a "cytoskeletal complex" that contained most of the platelets' actin and a high molecular weight (260,000 dalton) actin-binding protein (ABP) (26). Platelet ABP was originally named on the basis of its similar-

ities to the high molecular weight protein isolated from rabbit alveolar macrophages by Hartwig and Stossel (17, 47). Kane (22, 23) also described a high molecular weight (220,000 dalton) protein involved in the cross-linking of actin in sea urchin egg extracts into a solid birefringent gel. Subsequently, other high molecular weight actin-binding or gelation proteins have been identified in various nonmuscle cells (6, 11, 12, 19, 21, 31, 33, 43, 44, 49, 55). These proteins may or may not be similar to filamin isolated from smooth muscle and skeletal muscle sources (2, 45, 52, 54). ABPs and filamins from some of these sources show antibody cross-reactivity (14, 52, 54) and similar amino acid compositions (44, 52). In addition to these high molecular weight proteins, lower molecular weight actin cross-linking proteins have been purified from *Acanthamoeba* (29, 30) and Ehrlich ascites tumor cells (32).

In this paper we describe unique purification schemes for both ABP and actin from the platelet cytoskeleton whose in vitro recombination results in the formation of a structure remarkably similar to the platelets' native cytoskeleton, as visualized by negative staining. The reassembly of the platelet cytoskeleton from its purified components appears only to be affected by increasing ionic strength whereas, in the platelet lysates, increasing Ca^{+2} is found to disrupt the cytoskeleton. The regulation of the interaction between ABP and actin, in vivo, will undoubtedly be crucial to the understanding of several platelet processes such as shape change and filopodial formation.

MATERIALS AND METHODS

Acrylamide, *bis*-acrylamide, *N,N,N',N'*-tetramethylenediamine (TEMED), and glycine were obtained from Bio-Rad Laboratories, Inc. (Richmond, Calif.). Triton X-100 and PIPES were purchased from Calbiochem-Behring Corp. (LaJolla, Calif.). Leupeptin is a generous gift of Professor H. Umezawa of the Institute for Microbial Chemistry, Tokyo, Japan. EDTA, EGTA, SDS, ATP, and phenyl-methylsulfonyl fluoride (PMSF) are purchased from the Sigma Chemical Co. (St. Louis, Mo.). Polyethylene glycol 6000 (PEG-6000) is purchased from J. T. Baker Chemical Co. (Phillipsburg, N. J.) and DEAE-Sephacel is obtained from Pharmacia Fine Chemicals (Piscataway, N. J.).

Preparation of Platelets

Four units of human platelet concentrates were received ~3 h after the blood was drawn at the Greater New York Blood Center. The platelet-rich plasma was centrifuged at 350 *g* for 20 minutes to pellet any contaminating erythrocytes and leukocytes and was then spun at 1,000 *g* to pellet the platelets. The platelets were gently resuspended and washed twice by centrifugation in a solution containing 126 mM NaCl, 5 mM KCl, 0.3 mM EDTA, 10 mM NaPO₄, pH 7.4 (platelet wash). All utensils used in the platelet preparation were plastic or siliconized glass and all operations were carried out at 4°C.

Protein Purifications

Rabbit skeletal muscle actin were prepared according to the method of Spudich and Watt (46).

Platelet actin and ABP were prepared as described in the text.

Protein concentrations of column fractions were determined by using the Bio-Rad Coomassie Blue dye binding assay with γ-globulin as the standard. Alternatively, protein determinations were made by the method of Lowry et al. (25) using bovine serum albumin as the standard.

SDS PAGE

Samples to be electrophoresed were precipitated with 10% cold TCA and washed with acetone, if necessary (when precipitation is from Triton X-100 or PEG containing solutions). After neutralization with NH₄OH, the protein pellets were resuspended in 1% SDS, 1% 2-mercaptoethanol, 25 mM Tris-sulfate, pH 6.7, 0.002% bromophenol blue, 10% glycerol (gel sample buffer) and boiled for 2 min before applying to gel. The gels were 5.5% acrylamide, 25 mM Tris-glycine, pH 8.3, and were electrophoresed at 3 mA per gel in a running buffer of 25 mM Tris-glycine, pH 8.3. The gels were stained at 70°C with 0.1% Coomassie Brilliant

Blue in 30% propanol, 10% acetic acid, and were destained at 70°C in 7% acetic acid.

Polyacrylamide gels were scanned in a Quik-Scan densitometer (Helena Laboratories, Beaumont, Texas), the area under each peak being simultaneously monitored by an automatic integrator.

Electron Microscopy

To view the platelet cytoskeleton, a drop of cold Triton solubilization buffer (1% Triton X-100, 40 mM KCl, 10 mM imidazole-chloride, 10 mM EGTA, 2 mM NaN₃, pH 7.0) was added to a glow-discharged Formvar-coated grid followed by 1 μl of washed platelets resuspended 1:1 in the platelet wash. After a few minutes, the grid was washed with 40 mM KCl, 10 mM PIPES, 1 mM EGTA, 2 mM NaN₃, pH 6.8 (buffer A) and then negatively stained with 1% uranyl acetate.

Samples of purified platelet actin, ABP, or platelet actin followed by platelet ABP (conditions given in legend) were applied to glow-discharged Formvar-coated grids in buffer A. The grids were rinsed with buffer A and then negatively stained with 1% uranyl acetate.

RESULTS

Isolation of the Platelet Cytoskeleton

When washed human platelets were boiled in 1% SDS, 2-mercaptoethanol, and run on SDS polyacrylamide gels (Fig. 1, gel TP) the most striking feature observed was the preponderance of actin (42,500 mol wt). By quantitative densitometry, we previously determined (27) that actin makes up ~30% of the platelets' total protein. Another outstanding feature of this cell is the high molecular weight triplet. The lower band of the triplet is myosin heavy chain (subunit molecular weight, 200,000), the middle band (subunit molecular weight, 230,000) is as yet unknown, and the uppermost band (subunit molecular weight, 260,000) we named actin-binding protein (27). It is curious, and probably most significant, that actin and the proteins that bind to it constitute one half of the platelets' total protein (myosin = 12%, ABP = 8%) (27).

As washed platelets (resuspended 1:1 in platelet wash) are added to 10 vol of ice-cold 1% Triton X-100, 40 mM KCl, 10 mM imidazole-chloride, 10 mM EGTA, 2 mM NaN₃, pH 7.0 (Triton solubilization buffer), a flocculence appears immediately in the tube. This flocculent precipitate can be collected at 3,000 *g* (2 min) after settling for 12 min on ice. The Triton-
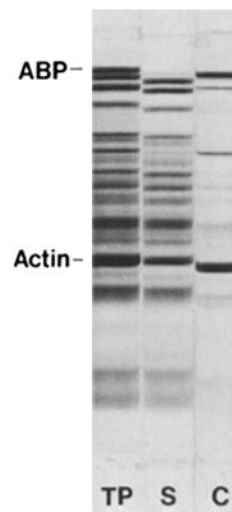

FIGURE 1 5.5% SDS PAGE of the cytoskeleton isolation. Stoichiometric loads of total platelets (*TP*), Triton-soluble platelet supernate after 3,000 *g* centrifugation (*S*), and Triton-X-100-insoluble cytoskeleton (*C*).

insoluble material is seen (Fig. 1, gel C) to be composed almost exclusively of actin, ABP, and a 105,000-dalton protein. Generally, this pellet contains 60–80% of the platelets' actin, 70–95% of the total ABP, and 90% of the 105,000-dalton protein. Conversely, the resulting supernate (gel S) is severely depleted of these three proteins. Various amounts of myosin may also be included in this pellet.

When platelets are treated with the Triton solubilization buffer directly on a carbon-coated grid, the results obtained are as seen in Fig. 2. Negative staining of the Triton-insoluble material reveals a structure with the correct size and shape for a resting platelet. In the absence of the membrane and the Triton-soluble cytoplasmic components, it is easy to visualize the branched bundles of filaments ~0.1–0.2 μm in diameter. The individual filaments resemble actin microfilaments in their dimensions. Microtubules are absent from this preparation, probably because of their depolymerization in the cold and subsequent solubilization by Triton.

Thus it appears that upon treatment with a Triton-EGTA solution, most of the platelets' components are solubilized with the exception of the platelet cytoskeleton—an easily sedimentable structure consisting mainly of ABP, actin, and the 105,000-dalton protein organized as microfilament bundles within the cell.

All of the components of the cytoskeleton-isolation solution are important. Omission of, or changes in the concentrations of any of the components, or the addition of new components can alter the composition or amount of the Triton-insoluble material.

Inclusion of 10 mM EDTA in the cytoskeletal-isolation solution would result in the formation of rigor bonds between myosin and the actin filaments of the platelet cytoskeleton and, consequently, more myosin would be included in the flocculent precipitate. We named this structure the "contractile appara-

tus" (28). Conversely, if MgATP had been added to the cytoskeleton isolation solution, the myosin seen here to be included in the cytoskeletal precipitate would have been absent.

If the concentration of KCl in the isolation solution is increased to >0.1 M, the recovery of ABP in the cytoskeletal complex is markedly reduced. This occurs because at higher salt concentrations, ABP becomes solubilized from the cytoskeleton and begins appearing in the supernate, as will be seen below.

The necessity for the high concentrations of EGTA in the isolation solution has two reasons. First, platelets have been shown to contain a Ca^{+2}-activated, sulfhydryl-dependent, neutral protease (41, 50). This protease is activated at 0.17 mM Ca^{+2} and has been shown to specifically attack ABP and the 230,000-dalton protein (50). If EGTA is omitted from the cytoskeleton isolation solution, the release of membrane-limited Ca^{+2} by Triton leads to the complete disappearance of these two proteins within 10 min on ice (Fig. 3, gel A). However, if platelets are diluted into increasingly larger volumes of the Triton solution, the Ca^{+2} levels can be lowered enough to prevent the proteolytic events (Fig. 3, gels B–G). This effect is indeed attributable to a decreased level of Ca^{+2} and not to a dilution-induced inactivation of the protease, because the addition of 1 mM $CaCl_2$ to the most dilute sample will result in extensive proteolysis (not shown). The final $[Ca^{+2}]$ in the platelet dilution showing the onset of proteolysis (Fig. 3, gel D) should be 0.17 mM, thereby allowing us to back calculate the $[Ca^{+2}]$ in the platelets to be ~51 mM.

The second reason for the high EGTA requirement for cytoskeletal isolation can be seen in Fig. 4. In this set of experiments platelets are added to Triton solubilization solutions with and without EGTA but including 100 μg/ml leupeptin, which is a potent inhibitor of the Ca^{+2}-activated protease (41). It can be seen (gel E) that very little cytoskeleton can be
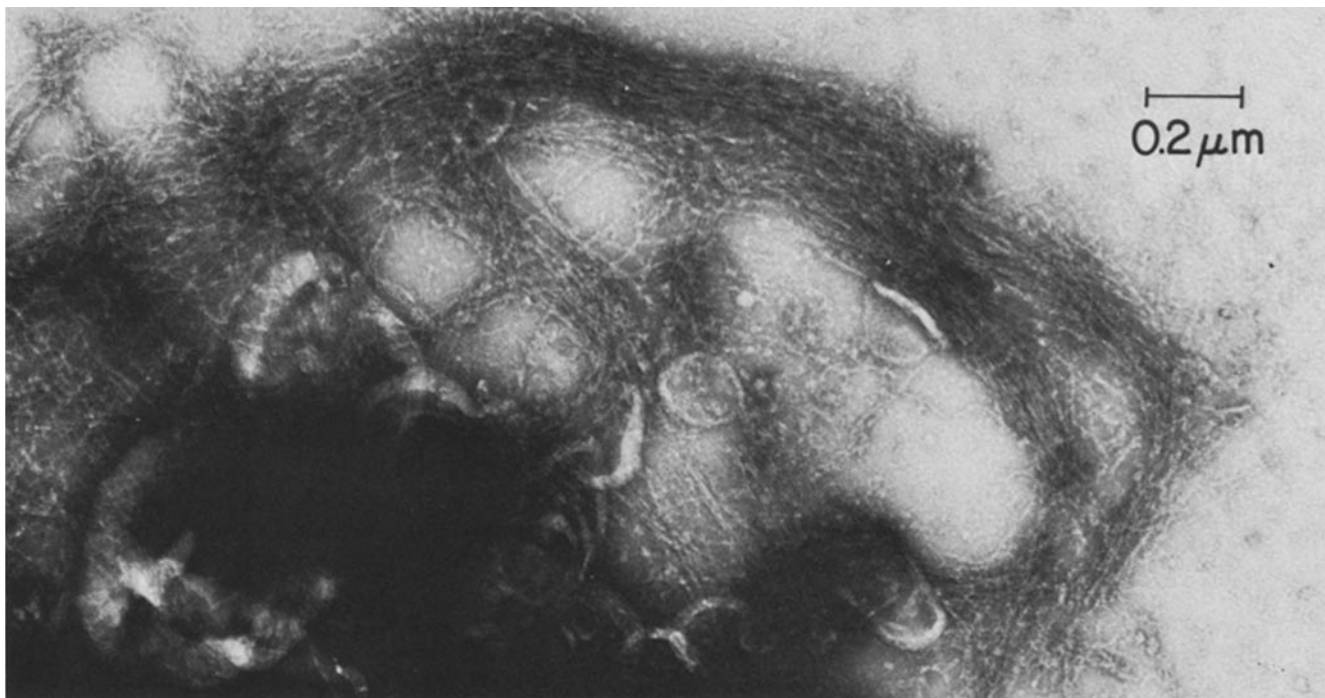

FIGURE 2   Resting discoid platelet (resuspended 1:1 in platelet wash) immersed in 10 vol of ice-cold Triton solubilization buffer (1% Triton X-100, 40 mM KCl, 10 mM EGTA, 10 mM imidazole-chloride, 2 mM NaN_3, pH 7.0) washed with buffer A and negatively stained with 1% uranyl acetate. Note the network of actin filament bundles comprising this Triton-X-100-insoluble platelet remnant. Bar, 0.2 μm. × 62,500.

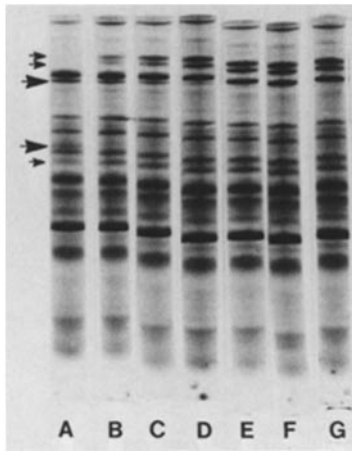Figure 3 5.5% SDS PAGE of Ca^{+2}-dependent protease turn-on point in platelet lysates. 10 μl of platelets (resuspended 1:1 in platelet wash) are added to (A) 0.1, (B) 0.75, (C) 1.0, (D) 1.5, (E) 2.0, (F) 3.0, and (G) 4.0 ml of Triton solubilization buffer without EGTA (1% Triton X-100, 40 mM KCl, 10 mM imidazole-chloride, 2 mM NaN₃, pH 7.0). After 12 min on ice, all samples are precipitated with 9 vol of cold acetone (1,000 g, 5 min). Acetone pellets are then brought to the same final volume in gel sample buffer and equal loads are electrophoresed. Small arrows point to the bands that disappear and large arrows point to those that appear upon proteolysis. Proteolysis is judged to begin in gel D by the appearance of the 190,000-dalton breakdown product and the reduction in staining of the 230,000-dalton protein. Therefore, if the [Ca^{+2}] in this 1.5-ml sample is 0.17 mM (protease turn-on point), all of the Ca^{+2} having been contributed by the 5 μl of platelets, the [Ca^{+2}] within the platelets is calculated to be 51 mM.
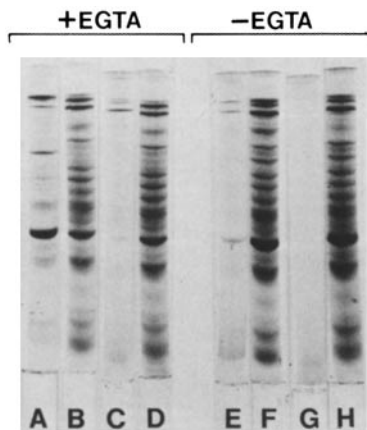

Figure 4 5.5% SDS PAGE of platelets added to the Triton solubilization buffer in the presence and absence of EGTA. 25 μl of 1:1 resuspended platelets are added to 250 μl of Triton solubilization buffer containing 10 mM EGTA (gels A–D) or without any EGTA (gels E–H). All solutions have a final concentration of 100 μg/ml of leupeptin to prevent proteolysis. Cytoskeletons are collected at 3,000 g (gels A and E) and the resulting supernates (gels B and F) are recentrifuged in an airfuge (Beckman Instruments Inc., Westbury, N.Y.) at 148,000 g (20 min). The high-speed pellets (gels C and G) and supernates (gels D and H) are shown. All gel loads are stoichiometric.

isolated in the absence of EGTA as compared with that in the presence of 10 mM EGTA (gel A) even though no proteolysis has occurred. Intact ABP remains in the low-speed supernate after Triton immersion (gel F). It may be noteworthy, however, that no 105,000-dalton protein is included in the small amount

of cytoskeleton that is isolated in the presence of Ca^{+2}. The 105,000-dalton protein may only be able to bind to the ABP-actin complex in the absence of Ca^{+2}.

Next, it was of interest to determine the state of the actin left behind in the low-speed Triton supernate. Because free F-actin filaments are soluble in 1% Triton (only cross-linked actin filaments, as by ABP, are Triton insoluble; unpublished observation), high-speed centrifugation was necessary to differentiate between F- and G-actin. It can be seen (Fig. 4, gels C and G) that little if any of the Triton-soluble actin sediments at 148,000 g, demonstrating that it is not in the filamentous state. Thus it appears that, in the presence of Ca^{+2}, not only is the cytoskeleton disrupted, but the uncomplexed actin is either depolymerized or fragmented into small oligomers that do not pellet at the speeds used. Alternatively, it may simply be that free actin filaments (perhaps as in gel B, or after ABP has been removed by a Ca^{+2}-directed event as in gel F) were more easily depolymerized when diluted 20-fold into the Triton solubilization solution.

Purification of ABP

The cytoskeleton isolated by the Triton-EGTA solubilization is washed once in the Triton-EGTA buffer and then twice in buffer A by resuspending and recentrifuging at 3,000 g for 2 min. The washed pellet is then resuspended in 0.6 M KCl, 10 mM PIPES, 2 mM NaN₃, pH 6.8 (high-salt buffer), homogenized for 2 min on ice, and clarified of high-salt-insoluble proteins at 25,000 g for 15 min (Fig. 5). Generally, the majority of the protein is solubilized by this procedure. The high-salt-soluble supernate is then brought to 5 mM in EGTA-ATP and stored for 16 h at 4°C. Kane (22) originally described the phenomenon that sea urchin egg actin forms birefringent bundles of filaments when ATP is added to a gelled extract solubilized by high salt. We find this to be the case with human platelet actin as well. When the high-salt/EGTA/ATP solution is centrifuged at 25,000 g (15 min), the pellet is seen to consist mostly of actin (Fig. 5, gel E), leaving the ABP behind in the supernate. This "bundling" step thereby provides a mechanism for easily separating actin from ABP once they are dissociated from each other in high salt. The actin bundles are used for the subsequent purification of actin while the bundle supernate is used for the preparation of ABP. 50% (wt/vol) PEG-6000 is added to this ABP-rich supernate until a final concentration of
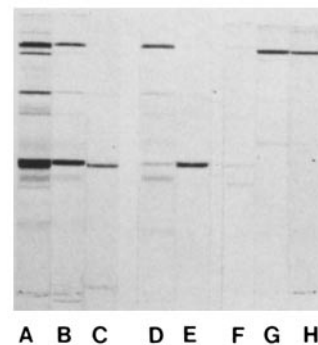

Figure 5 5.5% SDS PAGE of the initial ABP purification. Starting cytoskeleton (A), 25,000 g supernate (B), and pellet (C) after solubilization of the cytoskeleton in 0.6 M KCl. 25,000 g supernate (D) and pellet (E) after the "bundling" of actin in the high-salt-soluble fraction with EGTA-ATP. 10,000 g supernate (F) and pellet (G) after the precipitation of the bundle supernate with 5% PEG and the 5% PEG pellet resuspended and clarified (H).

5% is reached. After sitting for 10 min on ice, the solution is centrifuged at 10,000 g (12 min), sedimenting the ABP and separating it from most of its major contaminants (Fig. 5, gels F and G). The pellet is resuspended in buffer A minus KCl and its subsequent clarification (25,000 g, 30 min) usually removes the slight myosin contamination (Fig. 5, gel H). This PEG-purified ABP is generally found to be 90% pure when subjected to quantitative densitometry.

PEG-purified ABP is then applied to a DEAE-Sephacel column in 10 mM PIPES, 1 mM EGTA, 2 mM NaN₃, pH 6.8, and the adherent proteins are eluted with a linear KCl gradient (Fig. 6). ABP is seen to be eluted at ~0.2 M KCl, free of its contaminating proteins. The ABP peak is pooled, concentrated by dialysis against glycerol, and then dialyzed into buffer A. The yield of ABP during the purification is presented in Table I. The purified ABP can be stored for weeks in the refrigerator in 1 mM PMSF without any evidence of proteolysis or loss of its ability to bind to actin.

Purification of Platelet Actin

Two methods have been used to purify platelet actin. Actin-rich bundles (generated during the ABP purification) are resuspended in 0.6 M KCl, 10 mM PIPES, 2 mM NaN₃, pH 6.8, and rebundled overnight with 5 mM EGTA-ATP (Fig. 7). This process can be repeated several times, each time resulting in a further purification of the actin. Finally, the actin bundles are resuspended in buffer A, homogenized on ice, and centrifuged at 15,000 g (15 min) to pellet any actin complexes. The resulting supernate is seen to be highly purified actin. The pelleted actin can be redissolved in buffer A and recentrifuged to increase the yield of purified actin.

Alternatively, the actin-rich, high-salt-insoluble material generated during the ABP purification (Fig. 5, gel C) can be used to prepare actin. This pellet can be dissolved in and dialyzed against actin depolymerization buffer (2 mM Tris-

HCl, 0.2 mM CaATP, 0.5 mM 2-mercaptoethanol, pH 8.0). Actin is then purified through repeated cycles of polymerization and depolymerization according to Spudich and Watt (46).

The highly purified platelet actin is seen to retain its ability to self-associate into 25,000 g sedimentable bundles in 0.6 M KCl, 5 mM EGTA-ATP (Fig. 8). It is a unique observation that a mammalian actin can be bundled. Bryan and Kane (9) suggested that "actin bundling" is not a property common to all actins, because they were not able to bundle vertebrate skeletal muscle actin under identical conditions. We have confirmed their observation on rabbit skeletal muscle actin, which will not form bundles when treated in the same way as the platelet actin. Platelet actin has a critical concentration for bundling equal to 1.1 mg/ml in 5 mM EGTA-ATP as compared with sea urchin egg actin, which has a critical concentration for bundling of 1.2–1.3 mg/ml in 1 mM ATP (9).

The ability of the purified actin to bundle discounts the possibility that a contaminant in the high-salt extracts of the platelet cytoskeleton (e.g. the 105,000-dalton protein) was caus-

TABLE I
Recovery of ABP during Purification

Purification Step	% ABP recovered
Total platelet	100
Cytoskeleton	89
0.6 M KCl soluble cytoskeleton	62
Bundle supernate	57
5% PEG pellet	52
DEAE-Sephacel peak	36

The ABP purification was carried out as described in the text. At each stage of the purification, aliquots were removed and processed for SDS PAGE. Stoichiometric loads of the gel samples were electrophoresed, and the gels were scanned for their protein content. The % ABP recovered was a measure of the area under the ABP peak at each step of the purification compared with that in the total platelet. Results represent the average of five experiments.
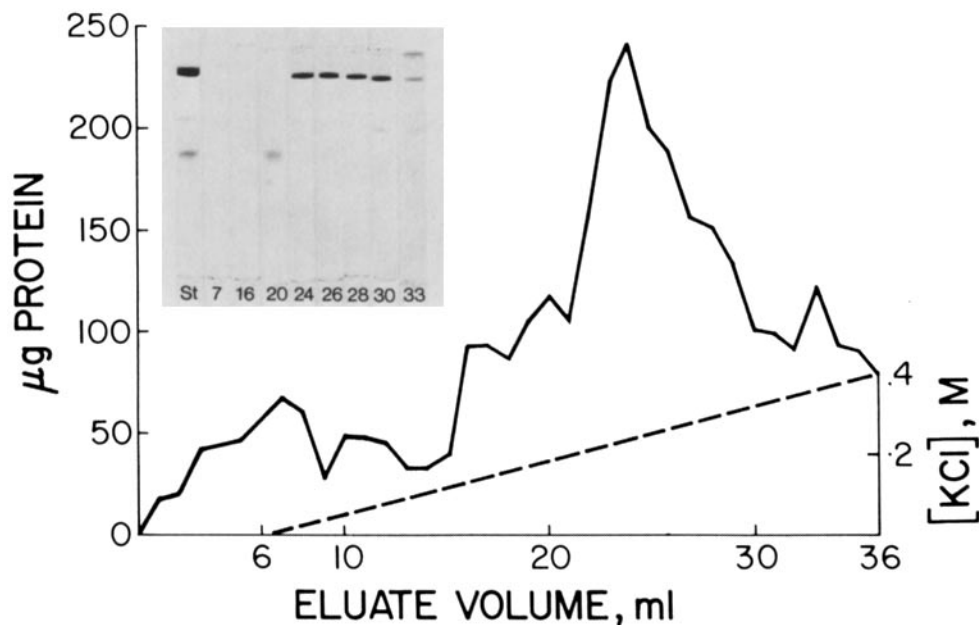

FIGURE 6 DEAE-Sephacel column purification of ABP. 3 mg of PEG-purified ABP are applied to a 0.7 × 5.0 cm DEAE-Sephacel column equilibrated with 10 mM PIPES, 1 mM EGTA, 2 mM NaN₃, pH 6.8. The column is washed with 2–3 column vol of this buffer and then eluted in 1-ml fractions with 30 ml of a 0–0.4 M KCl linear concentration gradient (prepared in PIPES-EGTA buffer). Protein concentrations are determined in every other fraction using the Bio-Rad dye binding assay. The dotted line represents the salt concentrations across the gradient. The inset shows 5.5% SDS polyacrylamide gels of selected column fractions and the starting material applied to the column (St).
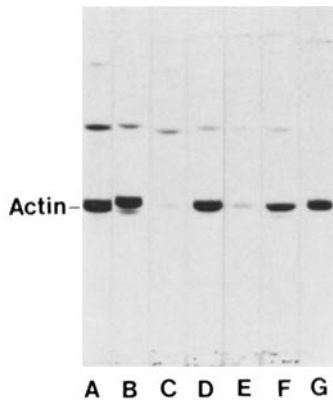
FIGURE 7 5.5% SDS PAGE of the platelet actin purification by bundling. Actin bundles (A), a by-product of the ABP purification (Fig. 5, gel E), are rebundled in 5 mM EGTA-ATP to yield a cleaner actin preparation (B) and its resultant supernate (C). These cleaner bundles are again cycled to yield another pellet (D) and supernate (E). The third bundle pellet is resuspended in buffer A, homogenized, and centrifuged at 15,000 g to yield a pellet (F) and a supernate (G) of purified actin.

ing the bundling and that it was not a property intrinsic to the actin itself.

Recombination of ABP and Actin In Vitro

When 25,000-g-clarified solutions of ABP and actin are added back together, in vitro, a flocculence forms immediately in the tube (Fig. 9). Upon agitation, the structure tightens and pulls away from the sides of the tube, exposing the fibrous nature of the network. No structures can be seen in the tubes containing ABP alone or actin alone subjected to the same treatment.

This filamentous structure can be sedimented at 5,000 g and the resulting supernate and pellet analyzed on SDS polyacrylamide gels. When PEG-purified ABP is used (Fig. 10), the minor contaminants associated with this starting material do not appear in the reformed cytoskeletal complex, suggesting that these proteins are not important in the reassociation reaction. This clearing out of contaminants upon in vitro formation of the cytoskeleton can be exploited as an alternative means of purifying the ABP. The reformed cytoskeletal complex is dissolved in 0.6 M KCl by soaking overnight and drawing up and down in a plastic pipette tip. Care must be taken to avoid losing protein by denaturation (because of vigorous repipetting) or by its sticking to the walls of the test tube or pipette tip. The solubilized ABP-actin complex is then centrifuged at 148,000 g, pelleting the F-actin and leaving the G-actin and ABP in the supernate (Fig. 10, gel E). ABP is separated from the G-actin by 5% PEG precipitation. A higher load of the ABP sample (Fig. 10, gel I) shows it to be highly purified.

The recombination experiment can also be followed by electron microscopy (Fig. 11). Negatively stained platelet actin filaments have a typical 7 nm diameter and appear to be randomly oriented. Negatively stained ABP appears as beaded coils or donuts, as described by Stossel and Hartwig (48). When these two proteins are added together on an EM grid the result is the alignment of the actin filaments into cables. Some free actin filaments can be seen, but most of them are arranged in parallel to form these thick cables. The supramolecular nature of this structure accounts for the low-speed sedimentability

(5,000 g) of the ABP-actin complex, formed from solutions that had previously been clarified at 25,000 g.

Rabbit skeletal muscle actin and platelet actin will both recombine with platelet ABP to form this cytoskeletal complex, provided that the actin is in the filamentous form. However, if G-actin (rabbit skeletal muscle or human platelet) is substituted for F-actin and if the combination with ABP is carried out in depolymerization buffer, no low-speed sedimentable complex will form. When G-actin is added to ABP in the presence of 2 mM $MgCl_2$, to induce the polymerization of the actin, the cytoskeletal complex forms immediately in the tube (Fig. 12). Therefore, it appears that ABP can form the low-speed sedimentable complex only with F-actin and not with G-actin.

When F-actin is used for the recombination, the cytoskeletal complex reforms rapidly at all temperatures tested (4°–37°C). Recombination of the purified components also appears to be independent of the presence or absence of divalent cations or ATP (data not shown). The Ca^{+2} sensitivity of the cytoskeletal assembly, which was present in the whole platelet, is lost upon the purification of its components.

The recombination of ABP and F-actin is, however, affected by the ionic strength of the solution in which recombination takes place. It can be seen in Fig. 13, that as the KCl concentration is increased, the amount of ABP pelleting in the cytoskeletal complex is decreased. Only after a significant amount of the ABP is solubilized does the actin begin to appear in the supernate as well. This is attributable to the ability of small amounts of ABP to bind up large amounts of actin. This high-salt solubility of the ABP-actin complex, seen here to result from the removal of ABP from the actin filaments, has been taken advantage of in the separation and purification of these platelet proteins.

DISCUSSION

Isolation of the Cytoskeleton

We believe that the platelet cytoskeleton as revealed in Fig. 2 lies in the ectoplasmic region just beneath the cell membrane, which excludes all platelet organelles. Morphological evidence for the attachment of actin filaments to platelet plasma membranes (58) and the presence of membrane contamination in
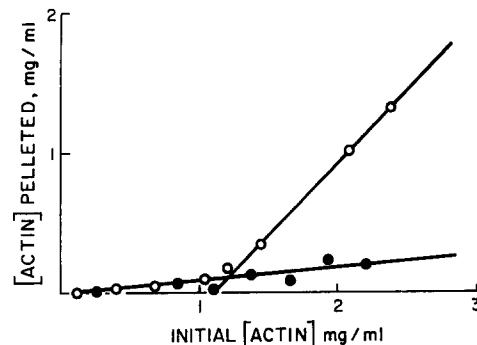

FIGURE 8 Actin bundling in high salt. Human platelet (open circles) and rabbit skeletal muscle actin (closed circles) are prepared as described in the text. Protein solutions are diluted to various starting actin concentrations in equal volumes of 0.6 M KCl and then EGTA-ATP is added to a final concentration of 5 mM. After 16 h at 4°C, the samples are centrifuged at 25,000 g for 15 min to pellet any newly formed bundles. Bundle pellets are resuspended in equal volumes of 0.6 M KCl and Lowry (26) protein determinations are performed on the bundle pellets and supernates as well as on the original actin dilutions to determine the extent of bundle formation.
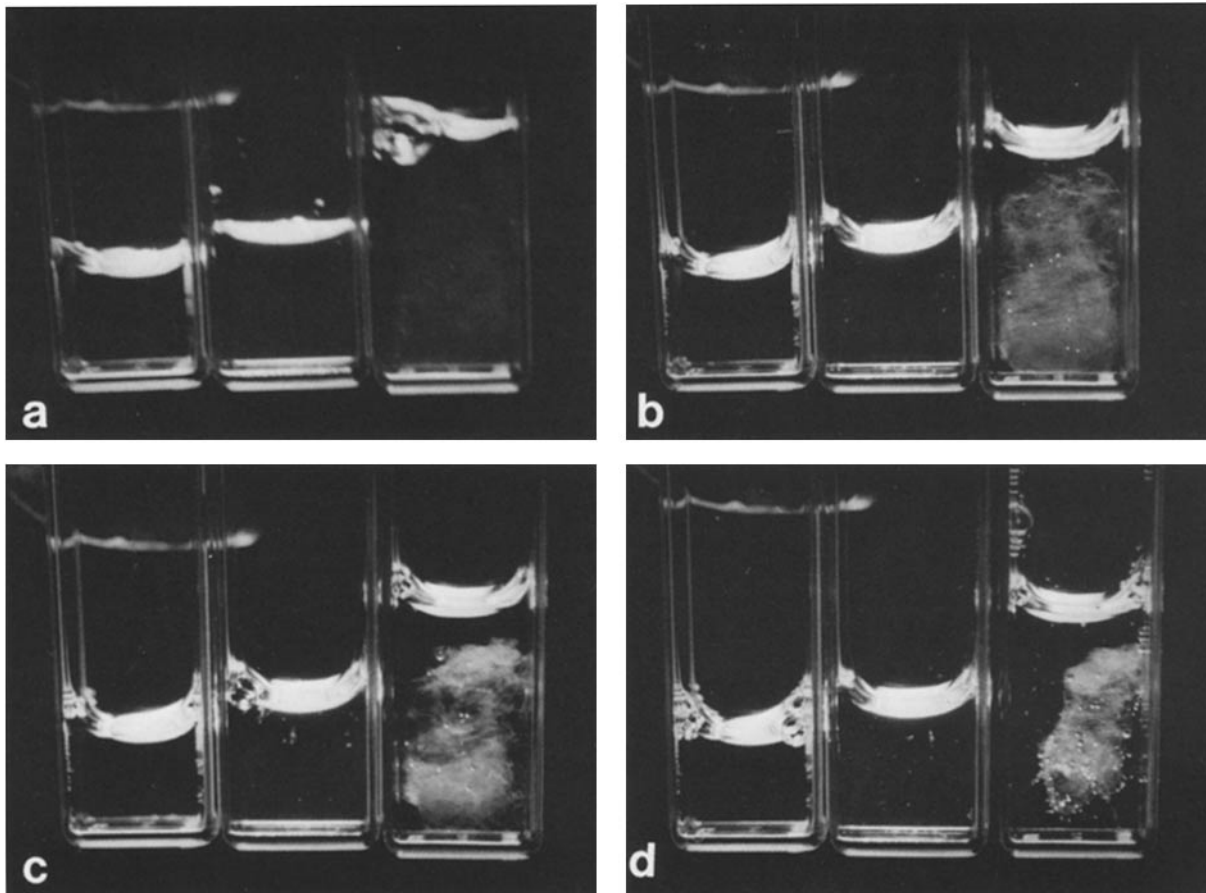
FIGURE 9   Recombination of ABP and F-actin, in vitro. In each panel, the first cuvette contains 0.8 ml of 3.2 mg/ml ABP, (in buffer A), the second cuvette has 1 ml of 1.84 mg/ml rabbit skeletal muscle F-actin (in 50 mM KCl, 2 mM MgCl₂) and the third cuvette has a combination of the first two. Panel a is photographed at time 0 after the addition of actin to ABP in buffer A. Panels b, c, and d are photographed 6, 8, and 10 min, respectively, after intermittent agitation of the tube.

crude platelet actomyosin preparations (40) suggest the close proximity of actin to the plasma membrane. Platelet membrane fractions were shown to contain a large amount of F-actin, which enhanced the MgATPase of muscle myosin by two- to threefold (13). Perhaps actin filaments have not been seen in the intact platelets' cortex by thin-section electron microscopy because they are bundled as twisted strands in a rope and therefore can never be in a proper plane of alignment to be seen in fixed and sectioned material.

Triton solutions have been used in the isolation of cytoskeletons since their introduction in 1976 by Brown et al. (8). In platelets, we find the cytoskeleton to consist mainly of ABP, actin, and 105,000-dalton protein (Fig. 1). The quantitative recovery of the 105,000-dalton protein from the platelet with the Triton solubilization buffer suggests that it is associated with the cytoskeleton in vivo even though it is not necessary for the in vitro interaction of purified ABP and actin (Fig. 9 and 11). Partially purified ABP and actin actually exclude the 105,000-dalton protein when forming the low-speed sediment-able ABP-actin complex (Fig. 10). We have achieved a partial purification of this protein and find that it comigrates with α-actinin on 5.5% SDS PAGE and cross-reacts with antibodies to α-actinin. It is different from α-actinin, though, in that its binding to actin appears to be Ca^{+2}-sensitive (S. Rosenberg, K. Burridge, and A. Stracher, manuscript in preparation). We can only speculate on the role of the 105,000-dalton protein in the platelet cytoskeleton. It may serve to link the ABP cross-linked actin filaments to sites beneath the plasma membrane, releasing
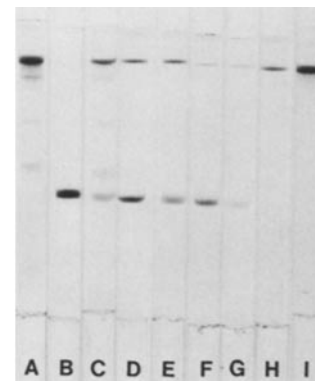

FIGURE 10   5.5% SDS PAGE of ABP and F-actin recombination, in vitro. 1.5 mg of PEG-purified ABP (A) is added to 0.83 mg of F-actin (doubled load) (B) in buffer A + 2 mM MgCl₂. After 15 min at room temperature, the solution is centrifuged at 5,000 g to yield a super-nate (C) and a pellet (D). Alternatively, the syneresed fluid can simply be decanted off. The pellet is resuspended in 0.6 M KCl, 10 mM PIPES, 2 mM NaN₃, pH 6.8, stored overnight and then spun in a Beckman airfuge at 148,000 g for 20 min to yield a supernate (E) and a pellet (F). The high-salt-soluble supernate is brought to 5% in PEG and sedimented at 10,000 g to yield a supernate (G) and a pellet (H). A higher load of the pellet is also shown (I).

them under conditions of Ca^{+2} flux to allow for the redistribution of the cytoskeletal components.

To preserve the cytoskeleton during the isolation procedure, it is essential to keep the concentration of calcium low. This
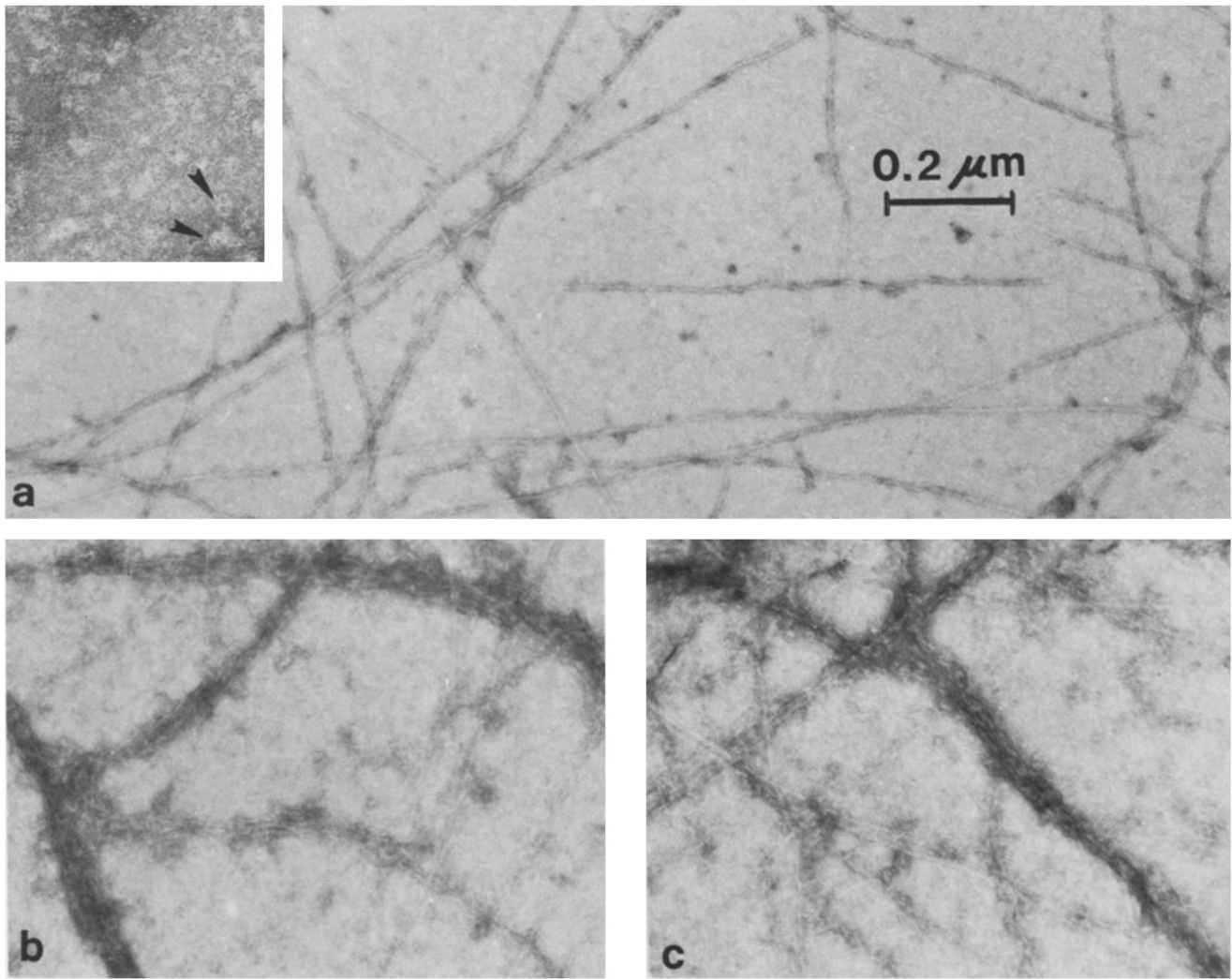
FIGURE 11 Recombination of platelet actin and ABP, in vitro. (a) Platelet F-actin (0.3 mg/ml, in 50 mM KCl, 2 mM MgCl₂) negatively stained with 1% uranyl acetate. *Inset* shows negatively stained ABP (note the absence of any filaments in this preparation) with arrows pointing out donutlike structures. *b* and *c* show platelet F-actin combined with ABP in buffer A (ABP: actin = 1:10 by weight) on an EM grid, washed with buffer A and stained with 1% uranyl acetate. The addition of ABP to actin, even at this low ratio, causes the normally random actin filaments to align themselves into cablelike structures. Bar, 0.2 µm. × 86,500; *inset*, × 112,100.
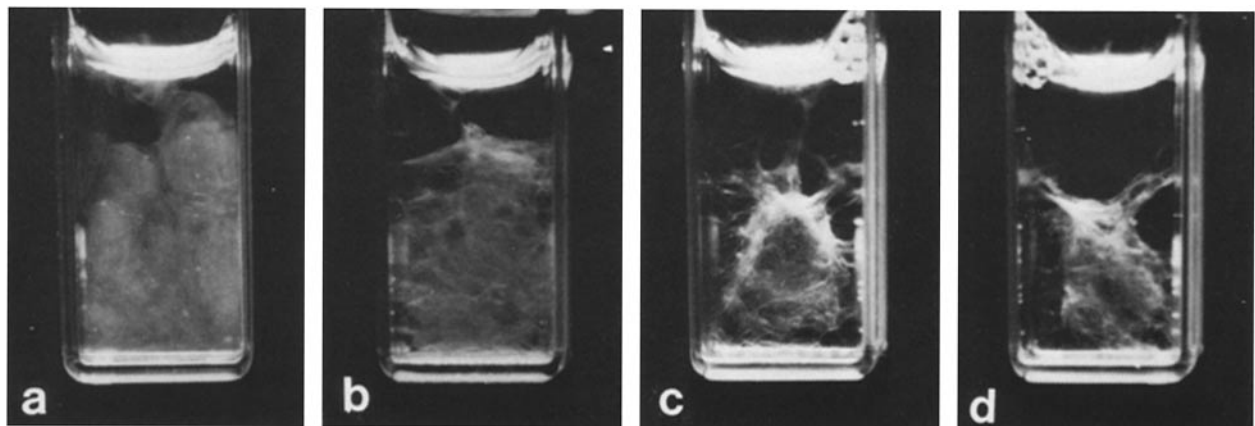

FIGURE 12 Recombination of ABP and G-actin, in vitro. 1.0 ml of 0.8 mg/ml platelet G-actin (in depolymerization buffer) is added to 1.0 ml of 3.0 mg/ml ABP in buffer A + 4 mM MgCl₂. Panel *a* is photographed at time 0 after the addition of the G-actin. Panels *b*, *c*, and *d* are photographed after intermittent agitation of the tube at 6, 8, and 10 min, respectively. Note how the structure in panels *a* and *b* comes to a small peak at the top; the actin began polymerizing and complexing with the ABP even before the pipette adding it could be removed from the tube and, upon withdrawal of the pipette, this small piece was pulled up.
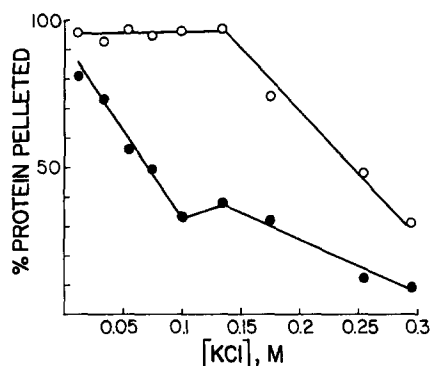
FIGURE 13 Effect of ionic strength on the recombination of ABP and actin, in vitro. 102 μg of skeletal muscle F-actin (final concentration, 0.41 mg/ml) is added to 88 μg of platelet ABP in solutions of increasing [KCl] (+ 10 mM PIPES, 0.3 mM MgCl₂, 0.12 mM EGTA, pH 6.8). After 15 min at room temperature, the ABP-actin complex is sedimented out at 5,000 g and the supernates are precipitated with cold 10% TCA. Gel samples are prepared and stoichiometric loads of the pellet and supernate are electrophoresed on SDS polyacrylamide gels. Gels are scanned in a Helena Quik-Scan densitometer equipped with an automatic integrater. Percent ABP in pellet (closed circles) and percent actin in pellet (open circles) are plotted against the KCl concentration.

requires a high concentration of EGTA, because the total free [Ca⁺²] within the platelet is determined from this study to be 51 mM (Fig. 3). The accuracy of this figure, however, is dependent upon the condition that the Ca⁺²-activated protease is turned on in the cell lysate at the same Ca⁺² level that the partially purified protease is turned on in vitro with ¹⁴C-casein as its substrate. The release of Ca⁺² from the platelets' membrane-enclosed dense bodies by the addition of Triton X-100 leads to the rapid breakdown (<10 min at 4°C) of ABP and the 230,000-dalton protein. At higher [Ca⁺²] (Fig. 3, gel A), an ~80,000 mol wt polypeptide begins to disappear. ABP proteolysis, however, is not the only reason for preventing the rise in free Ca⁺² upon cell lysis. As can be seen in Fig. 4, even when the proteolysis is inhibited by the inclusion of leupeptin in the Triton solubilization solution, no cytoskeletal complex can be isolated in the absence of 10 mM EGTA. This is not surprising, though, because in cell-free extracts prepared from other cell types (11, 12, 21, 22, 31, 43, 48, 55), the addition of micromolar concentrations of calcium prevents the formation of actin gels by actin-binding proteins upon warming of the extracts. The Ca⁺² must be exerting its effect indirectly on the ABP-actin cytoskeleton, perhaps through some other enzyme system in the platelet, because purified ABP and actin can reform the cytoskeletal network, in vitro, in the presence of millimolar calcium. The Ca⁺² sensitivity of this process in vivo, and its loss upon the purification of the components, is not an unprecedented phenomenon (7, 9, 31, 32).

Purification of ABP and Actin

Platelets serve as an excellent source for the preparation of ABP and actin because they contain large quantities of these two proteins. The key factors responsible for the high yields and purity of these preparations are (a) a near-quantitative recovery of ABP and actin in the first step (cytoskeletal isolation), (b) the solubility of the ABP-actin complex in high salt, and (c) the ability to bundle out the actin with EGTA-ATP, thus separating it from the ABP (Fig. 5). Because platelet actin

is found to have a critical concentration for bundling of 1.1 mg/ml (Fig. 8) the ABP-actin complex is resuspended in only a small volume of high-salt buffer, one to two times the volume of the original packed platelets, to keep the actin concentrated enough to bundle. The repeated bundling steps (Fig. 7) clear out the 105,000-dalton protein contaminant, which does not seem to bind well to the actin in high salt.

We have also introduced precipitation with PEG-6000 to the ABP purification. This may be responsible for enabling us to store the ABP for weeks in the refrigerator, in low salt, without encountering the extensive aggregation problem seen in some filamin preparations (45, 53) using ammonium sulfate fractionation. Also, because PEG fractionates essentially on the basis of molecular weight (20), we avoided the use of gel filtration chromatography. Care must be taken to exclude any F-actin from the sample to be PEG fractionated (because of incomplete bundling in the prior step), because its presence leads to irreversible clumping of the PEG precipitate.

The ability of partially purified ABP to rebind to actin and exclude its associated contaminants can be used as a type of biological affinity column for the further purification of the ABP (Fig. 10). The higher the ratio of ABP/actin used, the better the cleaning step. One problem encountered here, however, is that in order to squeeze the maximum amount of contaminants out of the reforming ABP-actin complex it is necessary to form a tight structure (either by tapping on the tube or by centrifugation). A tighter structure is more difficult to dissolve in the high-salt buffer and usually requires overnight soaking and gentle resuspension. Alternatively, the PEG-purified ABP is separated from its contaminants on a DEAE-Sephacel column (Fig. 6).

Recombination of ABP and Actin In Vitro

The re-formation of the cytoskeletal complex in vitro from purified components, occurs immediately on ice or at room temperature. At the molecular level, it is seen as the organization of random actin filaments into a more ordered network (Fig. 11). It is easy to imagine how this alignment of actin filaments can account for the platelets' cytoskeletal structure depicted in Fig. 2. At the gross morphological level, recombination of ABP and actin again shows an intricate meshwork of fibers (Figs. 9 and 12). The complexity of the structure formed is easily discerned with the unaided eye. No cations, chelators, nucleotides, or accessory proteins are necessary for the reassembly of this cytoskeleton in vitro. Only buffered KCl is present to keep the actin filamentous, since under actin-depolymerizing conditions the cytoskeleton does not reform. However, as the concentration of KCl is increased, the ABP-actin interaction is disrupted and the amount of sedimentable ABP-actin complex decreases (Fig. 13).

Recombination experiments are generally performed at high ratios of ABP/actin, because the effect of various factors on the binding of ABP to F-actin can be more easily discerned when working near the maximum binding ratio (1.3–1.4/1, ABP/actin by weight; S. Rosenberg and A. Stracher, manuscript in preparation). However, it is seen that even when only small amounts of ABP participate in the recombination reaction (e.g., at increasing [KCl], Fig. 13), large amounts of actin are still included in the low-speed sedimentable ABP-actin complex that forms. There is enough ABP in the platelet to account for the enlistment of all of the platelets' actin into the cytoskeletal structure.

Role of ABP and Actin in Platelet Activation

Newly formed filopodia of activated platelets are found to be replete with actin filaments aligned in parallel (57). Decoration with HMM subfragment 1 reveals that all of the actin filaments in the filopodia are of the same polarity, with arrowheads pointing in towards the body of the platelet (35). How do these filopodia form after the platelets are stimulated? What regulates the movement of actin into these structures?

Filopodia are thought to form by either one of two mechanisms: (a) polymerization of cytoplasmic G-actin into filaments pushing out the filopodia, or (b) from preformed actin filaments that move out from the body of the platelet. Because we find the majority of the platelets' actin to be in the filamentous form, associated with ABP in the cytoskeleton (Fig. 1), we propose that the latter mechanism occurs.

These results differ from those of others who find the majority of the platelets' actin to be in a nonfilamentous form (10, 34, 42). The differences in our finding must lie in the Triton solubilization solutions that we use. Our solution has a higher EGTA concentration designed to chelate the calculated 51 mM Ca^{+2} in platelets, lower ionic strength, and lower pH, and the solubilization is performed at a lower temperature. We have shown that high ionic strength (Fig. 13) and Ca^{+2} (Fig. 4) will disrupt the formation of the cytoskeleton, and Carlsson et al. (10) have also described a Ca^{+2}-induced depolymerization of the platelets' actin. Therefore, it is possible that the differences in our Triton solutions are enough to account for the differences in results. If anything, our Triton solutions' low ionic strength and temperature and lack of divalent cations would cause the depolymerization of actin—not its polymerization.

Platelet activation may occur in a fashion analogous to coelomocyte transformation from petaloid to filopodial cells. These cells, described by Edds (15, 16), function as platelets in the sea urchin where they send out filopodia and retract clots to plug wounds. Actin filaments, which are randomly oriented in the petaloid (resting) cell, are repositioned upon activation into a radial orientation. Bundles of filaments form and these go on to form larger bundles that eventually become the axial support for each filopodium.

The disassembly of the platelet cytoskeleton to allow for the reorganization of actin filaments, and its reassembly after filopodial formation, can all be under the control of micromolar levels of intracellular Ca^{+2}. Nachmias (36, 37) has shown that filopodial formation can be arrested when platelets are treated with local anesthetics. Concomitant with the irreversible suppression of filopodial formation is the proteolysis of ABP. Because local anesthetics displace Ca^{+2} from cell membranes (18, 24), she suggested that the activation of the Ca^{+2}-dependent protease could be responsible for the degradation of the ABP. We have shown that the heavy fragment of proteolyzed ABP (HF-1, ABP molecular weight = 190,000) can bind to but not cross-link actin filaments (51). Therefore, her data provide excellent evidence that intact, functional ABP is an absolute requirement for filopodial formation. Using lower concentrations of anesthetics, however, Nachmias observed no ABP proteolysis, and the filopodial suppression could be reversed by washing out the anesthetic (36, 37). Perhaps at the lower anesthetic concentrations, less Ca^{+2} was displaced so that the free calcium level within the platelet still rose but not to the level necessary to cause proteolysis. As we have shown in Fig. 4, the cytoskeleton is disrupted under conditions of increased $[Ca^{+2}]$ in the absence of proteolysis. Nicholson et al. (38, 39) presented morphological evidence that local anesthetics cause dramatic changes in cell shape and cytoskeletal organization. They proposed Ca^{+2} displacement from the membrane as the cause of membrane blebbing and a destabilization of the microfilaments beneath the plasma membrane, uncoupling any cooperation between them (38).

Therefore, ABP appears to play a crucial role in filopodial formation in relation to its association with or dissociation from actin. We postulate that the state of assembly of these two proteins can be controlled by calcium fluxes in the platelet in vivo, i.e., during platelet activaton.

REFERENCES

1. Adelstein, R. S., and T. D. Pollard. 1978. Platelet contractile proteins. *Prog. Hemostasis Thromb.* 4:37–58.
2. Bechtel, P. J. 1979. Identification of a high molecular weight actin-binding protein in skeletal muscle. *J. Biol. Chem.* 254:1755–1758.
3. Behnke, O., B. I. Kristensen, and L. Engdahl Nielsen. 1971. Electron microscopical observations on actinoid and myosinoid filaments in blood platelets. *J. Ultrastruct. Res.* 37:351–369.
4. Bettex-Galland, M., and E. F. Lüscher. 1959. Extraction of an actomyosin-like protein from human thrombocytes. *Nature (Lond.).* 184:276–277.
5. Bettex-Galland, M., H. Portzehl, and E. F. Lüscher. 1962. Dissociation of thrombosthenin into two components comparable with actin and myosin. *Nature (Lond.).* 193:777–778.
6. Boxer, L. A., and T. P. Stossel. 1976. Interaction of actin, myosin and an actin-binding protein of chronic myelogenous leukemia leukocytes. *J. Clin. Invest.* 57:964–976.
7. Brotschi, E. A., J. H. Hartwig, and T. P. Stossel. 1978. The gelation of actin by actin-binding protein. *J. Biol. Chem.* 253:8988–8993.
8. Brown, S., W. Levinson, and J. A. Spudich. 1976. Cytoskeletal elements of chick embryo fibroblasts revealed by detergent extraction. *J. Supramol. Struct.* 5:119–130.
9. Bryan, J., and R. E. Kane. 1978. Separation and interaction of the major components of sea urchin actin gel. *J. Mol. Biol.* 125:207–224.
10. Carlsson, L., F. Markey, I. Blikstad, T. Persson, and U. Lindberg. 1979. Reorganization of actin in platelets stimulated by thrombin as measured by the DNase I inhibition assay. *Proc. Natl. Acad. Sci. U. S. A.* 76:6376–6380.
11. Clark, T. G., and R. W. Merriam. 1978. Actin in *Xenopus* oocytes. I. Polymerization and gelation in vitro. *J. Cell Biol.* 77:427–438.
12. Condeelis, J. S., and D. L. Taylor. 1977. The contractile basis of ameboid movement. V. The control of gelation, solation and contraction in extracts from *Dictyostelium discoideum.* *J. Cell Biol.* 74:901–927.
13. Crawford, N. 1976. Platelet microfilaments and microtubules. *In* Platelets in Biology and Pathology. J. L. Gordon, editor. Elsevier/North Holland Biomedical Press, Amsterdam. 121–157.
14. Davies, P., Y. Shizuta, K. Olden, M. Gallo, and I. Pastan. 1977. Phosphorylation of filamin and other proteins in cultured fibroblasts. *Biochem. Biophys. Res. Commun.* 74: 300–307.
15. Edds, K. T. 1977. Dynamic aspects of filopodial formation by reorganization of microfilaments. *J. Cell Biol.* 73:479–491.
16. Edds, K. T. 1979. Isolation and characterization of two forms of a cytoskeleton. *J. Cell Biol.* 83:109–115.
17. Hartwig, J. H., and T. P. Stossel. 1975. Isolation and properties of actin, myosin and a new actin-binding protein in rabbit alveolar macrophages. *J. Biol. Chem.* 250:5696–5705.
18. Hauser, H., and R. M. C. Dawson. 1968. The displacement of calcium ions from phospholipid monolayers by pharmacologically active and other organic bases. *Biochem. J.* 109:909–916.
19. Heggeness, M. H., K. Wang, and S. J. Singer. 1977. Intracellular distributions of mechanochemical proteins in cultured fibroblasts. *Proc. Natl. Acad. Sci. U. S. A.* 74:3883–3887.
20. Ingham, K. C. 1978. Precipitation of proteins with polyethylene glycol: characterization of albumin. *Arch. Biochem. Biophys.* 186:106–113.
21. Ishiura, M., and Y. Okada. 1979. The role of actin in temperature-dependent gel-sol transformation of extracts of Ehrlich ascites tumor cells. *J. Cell Biol.* 80:465–480.
22. Kane, R. E. 1975. Preparation and purification of polymerized actin from sea urchin egg extracts. *J. Cell Biol.* 66:305–315.
23. Kane, R. E. 1976. Actin polymerization and interaction with other proteins in temperature-induced gelation of sea urchin egg extracts. *J. Cell Biol.* 71:704–714.
24. Low, P. S., D. H. Lloyd, T. M. Stein, and J. A. Rogers III. 1979. Calcium displacement by local anesthetics. *J. Biol. Chem.* 254:4119–4125.
25. Lowry, O. H., N. J. Rosebrough, A. L. Farr, and R. J. Randall. 1951. Protein measurement with the Folin phenol reagent. *J. Biol. Chem.* 193:265–275.
26. Lucas, R. C., T. C. Detwiler, and A. Stracher. 1976. The identification and isolation of a high molecular weight (270,000 dalton) actin-binding-protein from human platelets. *J. Cell Biol.* 70 (2, Pt, 2):259 a (Abstr.).
27. Lucas, R. C., M. Gallagher, and A. Stracher. 1976. Actin and actin-binding-protein in platelets. *In* Contractile Systems in Non-Muscle Tissues. S. V. Perry, A. Margreth, and R. S. Adelstein, editors. North Holland Publishing, New York. 133–139.
28. Lucas, R. C., S. Rosenberg, S. Shafiq, A. Stracher, and J. Lawrence. 1979. The isolation and characterization of a cytoskeleton and a contractile apparatus from human platelets. *In* Protides of the Biological Fluids. H. Peeters, editor. Pergamon Press, New York. 465–470.
29. MacLean-Fletcher, S. D., and T. D. Pollard. 1980. Viscometric analysis of the gelation of *Acanthamoeba* extracts and purification of two gelation factors. *J. Cell Biol.* 85:414–428.
30. Maruta, H., and E. D. Korn. 1977. Purification from *Acanthamoeba castellanii* of proteins

that induce gelation and syneresis of F-actin. *J. Biol. Chem.* 252:399–402.

31. Mimura, N., and A. Asano. 1978. Actin-related gelation of Ehrlich tumour cell extracts is reversibly inhibited by low concentrations of Ca^{+2}. *Nature (Lond.).* 272:273–276.

32. Mimura, N., and A. Asano. 1979. Ca^{+2}-sensitive gelation of actin filaments by a new protein factor. *Nature (Lond.).* 282:44–48.

33. Moore, P. B., D. R. Anderson, J. W. Huggins, and K. L. Carraway. 1976. Cytoskeletal proteins associated with cell surface envelopes from sarcoma 180 ascites tumor cells. *Biochem. Biophys. Res. Commun.* 72:288–294.

34. Nachmias, V. T. 1980. Cytoskeleton of human platelets at rest and after spreading. *J. Cell Biol.* 86:795–802.

35. Nachmias, V. T., and A. Asch. 1976. Regulation and polarity: results with myxomycete plasmodium and with human platelets. *In* Cell Motility. R. Goldman, T. Pollard, and J. Rosenbaum, editors. Cold Spring Harbor Laboratory Conference on Cell Proliferation, Cold Spring Harbor, New York. 771–783.

36. Nachmias, V. T., J. S. Sullender, and A. Asch. 1977. Shape and cytoplasmic filaments in control and lidocaine-treated human platelets. *Blood.* 50:39–53.

37. Nachmias, V. T., J. S. Sullender, and J. R. Fallon. 1979. Effects of local anesthetics on human platelets: filopodial suppression and endogenous proteolysis. *Blood.* 53:63–72.

38. Nicholson, G. L., and G. Poste. 1976. Cell shape changes and transmembrane receptor uncoupling induced by tertiary amine local anesthetics. *J. Supramol. Struct.* 5:65–72.

39. Nicholson, G. L., J. R. Smith, and G. Poste. 1976. Effects of local anesthetics on cell morphology and membrane-associated cytoskeletal organization in BALB/3T3 cells. *J. Cell Biol.* 68:395–402.

40. Niederman, R., and T. D. Pollard. 1975. Human platelet myosin. II. In vitro assembly and structure of myosin filaments. *J. Cell Biol.* 67:72–92.

41. Phillips, D. R., and M. Jakabova. 1977. Ca^{+2}-dependent protease from human platelets. *J. Biol. Chem.* 252:5602–5605.

42. Phillips, D. R., L. K. Jennings, and H. H. Edwards. 1980. Identification of membrane proteins mediating the interaction of human platelets. *J. Cell Biol.* 86:77–86.

43. Pollard, T. D. 1976. The role of actin in the temperature-dependent gelation and contraction of extracts of *Acanthamoeba. J. Cell Biol.* 68:579–601.

44. Schloss, J. A., and R. D. Goldman. 1979. Isolation of a high molecular weight actin-binding protein from baby hamster kidney (BHK-21) cells. *Proc. Natl. Acad. Sci. U. S. A.* 76: 4484–4488.

45. Shizuta, Y., H. Shizuta, M. Gallo, P. Davies, I. Pastan, and M. S. Lewis. 1976. Purification and properties of filamin, an actin binding protein from chicken gizzard. *J. Biol. Chem.* 251:6562–6567.

46. Spudich, J. A., and S. Watt. 1971. The regulation of rabbit skeletal muscle contraction. I. Biochemical studies of the interaction of the tropomyosin-troponin complex with actin and the proteolytic fragments of myosin. *J. Biol. Chem.* 246:4866–4871.

47. Stossel, T. P., and J. H. Hartwig. 1975. Interactions between actin, myosin and an actin-binding protein from rabbit alveolar macrophages. *J. Biol. Chem.* 250:5706–5712.

48. Stossel, T. P., and J. H. Hartwig. 1976. Interactions of actin, myosin and a new actin-binding protein of rabbit pulmonary macrophages. II. Role in cytoplasmic movement and phagocytosis. *J. Cell Biol.* 68:602–619.

49. Taylor, D. L., J. A. Rhodes, and S. A. Hammond. 1976. The contractile basis of ameboid movement. II. Structure and contractility of motile extracts and plasmalemma-ectoplasm ghosts. *J. Cell Biol.* 70:123–143.

50. Truglia, J. A., A. Stracher, and R. C. Lucas. 1978. Proteolysis of human platelet cytoskeleton by endogenous Ca^{+2}-dependent protease. *Fed. Proc.* 37:1790a (Abstr.).

51. Truglia, J. A., A. Stracher, and R. C. Lucas. 1979. Human platelet cytoskeleton is proteolyzed by an endogenous Ca^{+2}-dependent protease. *Fed. Proc.* 38:1262a (Abstr.).

52. Wallach, D., P. J. A. Davies, and I. Pastan. 1978. Purification of mammalian filamin. *J. Biol. Chem.* 253:3328–3335.

53. Wang, K. 1977. Filamin, a new high-molecular-weight protein found in smooth muscle and nonmuscle cells. Purification and properties of chicken gizzard filamin. *Biochemistry.* 16:1857–1865.

54. Wang, K., J. F. Ash, and S. J. Singer. 1975. Filamin, a new high-molecular-weight protein found in smooth muscle and non-muscle cells. *Proc. Natl. Acad. Sci. U. S. A.* 72:4483–4486.

55. Weihing, R. R. 1976. Cytochalasin B inhibits actin-related gelation of HeLa cell extracts. *J. Cell Biol.* 71:303–307.

56. White, J. G. 1971. Platelet morphology. *In* The Circulating Platelet. S. A. Johnson, editor. Academic Press, Inc., New York. 45–121.

57. Zucker-Franklin, D. 1969. Microfibrils of blood platelets: their relationship to microtubules and the contractile protein. *J. Clin. Invest.* 48:165–175.

58. Zucker-Franklin, D. 1970. The submembranous fibrils of human blood platelets. *J. Cell Biol.* 47:293–299.